

## A HIGH PERFORMANCE SENSOR FOR HEAT-FLUX DIFFERENTIAL SCANNING CALORIMETRY \*

G. VAN DER PLAATS

*Anatech b.v., Pissummerweg 1, 6114 AH Susteren (The Netherlands)*

T. KEHL

*Mettler Instrumente, Im Langacher, 8606 Greifensee (Switzerland)*

(Received 26 January 1990)

### ABSTRACT

A new sensor for heat-flux differential scanning calorimetry is introduced. A description is given of the construction of the sensor, the specifications are discussed and an illustration is given of the performance of the sensor.

### INTRODUCTION

In heat-flux differential scanning calorimetry, the measured signal consists of the temperature difference  $\Delta T$  between sample and reference, both being subjected to a certain temperature–time profile. The sensor with which this temperature difference is measured, basically a differential thermocouple, determines the quality of the resulting signal to a very high degree.

The relationship between heat-flow  $dq/dt$  and  $\Delta T$  is (though approximate, but very clearly) given by [1]

$$\Delta T = (\Delta K_T / K_T) + (\Delta C_{SR} / K_T)(dT/dt) - (C_S / K_T)[d(\Delta T)/dt] - (1/K_T)(dq/dt) \quad (1)$$

Here,

$$\Delta K_T = (K_{1S} - K_{1R})(T_f - T) + (K_{2S} - K_{2R})(T_f^4 - T^4) + (K_{3S} - K_{3R})(T_f - T) \quad (2)$$

\* Presented at the 18th Annual NATAS Conference, San Diego, CA, U.S.A., 24–27 September 1989.

and

$$K_T = K_{1S} + K_{3S} + 2K_{4SR} + 4(K_{2S} + 2K_{5SR})T^3 \quad (3)$$

In these equations,  $K_{1S}$  and  $K_{1R}$  represent the coefficients of conductive heat-transfer between furnace and sample (reference),  $K_{2S}$  and  $K_{2R}$  the coefficients of radiative heat-transfer between furnace and sample (reference),  $K_{3S}$  and  $K_{3R}$  the coefficients of heat-transfer through sample and reference thermocouple wires,  $K_{4SR}$  represents the coefficient of conductive heat-transfer between sample and reference, and  $K_{5SR}$  the coefficient of radiative heat-transfer between sample and reference. Further,  $C_S$  denotes the heat capacity of the sample,  $\Delta C_{SR}$  the difference in heat capacity between sample and reference,  $T_f$  the furnace temperature and  $T$  the reference temperature.  $\Delta K_T$  can be regarded as a term defining the symmetry of the measuring cell and  $K_T$  as an overall heat-transfer coefficient.

The curve resolution of the sensor is defined by

$$\Delta T = \Delta T_{\max} \exp\left[(-K_T/C_S)t\right] \quad (4)$$

It follows clearly from eqns. (1) and (4) that an optimal design of a heat-flux DSC sensor features a high value of  $K_T$ . Unfortunately, as eqn. (1) also shows, the measured  $\Delta T$  signal decreases with increasing values of  $K_T$ , leading to low signal-to-noise ratios. This places heat-flux differential scanning calorimetry in a dilemma: on the one hand a high  $K_T$  value improves the quality of the measured signal, while on the other hand it lowers that quality. In practice, two constructive extremes exist: first, a sensor with a low  $K_T$  value leading to a high output and a low curve resolution; and second, a sensor with a high  $K_T$  value resulting in a low output and a high curve resolution. All existing sensors can be classified into one of these groups.

A new sensor for heat-flux differential scanning calorimetry has now been developed featuring both a high output and a high curve resolution.

## DESCRIPTION

The sensor basically consists of a supporting disc on the surface of which a multi-element thermopile is mounted.

The supporting disc serves for conduction of the heat flow from the furnace to the sample and reference. In order to obtain a high  $K_T$  value, the material of the disc needs to have a high heat conductivity. This limits the choice of suitable materials to metals and some ceramics such as  $\text{Al}_2\text{O}_3$  and boron nitride (BN). As the electrical conductivity of metals is a serious disadvantage here and as the mechanical properties of BN are rather poor, alumina was selected as the material for the supporting disc. A problem with this material is its extreme hardness, which makes conventional machining difficult. However, owing to the availability of high-power laser machining

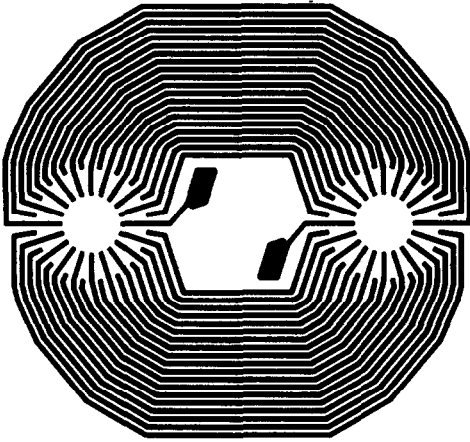


Fig. 1. Sensor lay-out.

techniques, this material also can be shaped with very high accuracy. Using these and other techniques, very well-defined thermal resistances are obtained in the disc, with the aim of increasing the quantitative behaviour and reproducibility.

On the surface of the supporting disc a multi-element thermopile is mounted. Here, use was made of thick-film screen-printing techniques featuring a very high positioning accuracy and allowing very narrow (down to  $75\ \mu\text{m}$ ) and thin (down to  $5\ \mu\text{m}$ ) traces to be applied. Normally, combinations of metals and ceramics can be applied only in a very limited temperature range, owing to the considerable differences in thermal expansion coefficient between these materials. Here however, as a result of the very thin layers and the use of a specially developed screen-printing paste, bonding which is stable over a wide temperature range could be achieved. In this way it became possible to position as many as 40 thermoelements in a sample sensing area with a diameter of only 5 mm, all connected in series to 40 identical thermoelements in the reference sensing area. A part of the sensor lay-out is given in Fig. 1.

Gold and a gold/palladium alloy were selected as thermocouple materials. This combination features a thermoelectric output of  $40\ \mu\text{V K}^{-1}$  and proved to have a perfect long time stability. Consequently, the sensor output amounts to more than  $1500\ \mu\text{V K}^{-1}$ !

The thermopile is electrically insulated with a thin, non-porous ceramic layer, allowing the sample and reference crucible to be placed directly onto the sensing areas. The distance between crucible and thermopile is therefore of the order of a few  $\mu\text{m}$  as a result of which the total thermal resistance is kept very low (approx.  $30\ \text{K W}^{-1}$ ). Together with the very low thermal capacity of the system this leads to a signal time constant of less than 2.5 s (measured with a 5 mg In sample in a normal Al crucible) and a calorimetric sensitivity of approx.  $50\ \mu\text{V mW}^{-1}$ . This value, combined with a signal

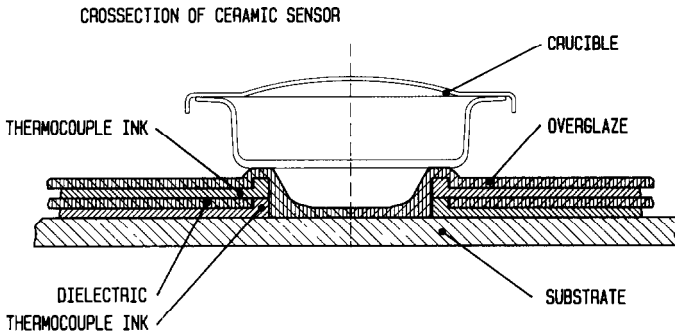


Fig. 2. Schematic cross-section of the sensor.

amplifier with a noise level of 50 nV peak–peak, leads to an extremely low thermal noise level of approx. 1  $\mu\text{W}$  peak–peak!

A schematic cross section of the sensor is given in Fig. 2. It can be clearly seen that the thermopile is constructed such that all thermoelements protrude to some extent from the surface of the supporting disc. In this way, the thermopile forms an integral part of the heat-flow path from furnace to sample and reference. This considerably enhances the quantitative performance of the sensor.

The temperature stability of this new sensor is excellent. As stated before, this results from the thin metal traces used and the special bonding mechanism of the applied screen-printing paste. The sensor therefore can be used easily in a temperature range from  $-150^{\circ}\text{C}$  up to  $800^{\circ}\text{C}$ . Moreover, the thermoshock stability is also outstanding. Cooling rates of more than  $1000\text{ K min}^{-1}$  (achieved by putting the sensor directly into liquid nitrogen) are easily withstood.

As the surface of the sensor consists of a non-porous ceramic material and gold wires are used for the connection to the signal amplifier both the chemical and the mechanical resistance of the sensor are high. The sensor can be used without any problems in very reactive standing atmospheres ( $\text{HCl}$ ,  $\text{NO}_x$ ), and even withstands immersion in concentrated  $\text{HNO}_3$  for several days.

## SPECIFICATIONS

The specifications of the newly developed sensor can be summarized as follows:

temperature range	$-150^{\circ}\text{C}$ to $+800^{\circ}\text{C}$
signal time constant	approx. 2.5.s
calorimetric sensitivity	approx. $50\ \mu\text{V mW}^{-1}$
chemical resistance	+++
mechanical resistance	+++

## PERFORMANCE

The high performance of this sensor can best be illustrated with some examples. Here, the sensor was mounted in a Mettler DSC 25 measuring cell. In Fig. 3 a baseline is given in the temperature range between  $-150^{\circ}\text{C}$  and  $+750^{\circ}\text{C}$ . Also as a result of the heat-flux measuring principle, very flat, linear and reproducible baselines over a large temperature range are easily possible.

Figure 4 shows a measurement of 2.382 mg of octacosane, a substance featuring polymorphic behaviour. The DSC curve shows two peaks with a separation of only  $4^{\circ}\text{C}$ . It can clearly be seen that a good peak resolution exists even with a high heating rate of  $20^{\circ}\text{C min}^{-1}$ .

Finally, Fig. 5 shows the heating curve of a strong polyethylene fibre. Owing to the very linear orientation of the polymer chains the melting

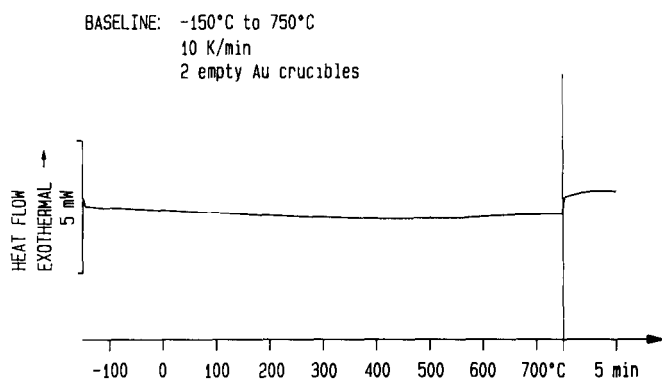


Fig. 3. Baseline from  $-150^{\circ}\text{C}$  to  $+750^{\circ}\text{C}$ ,  $10\text{ K min}^{-1}$ , two empty Au crucibles.

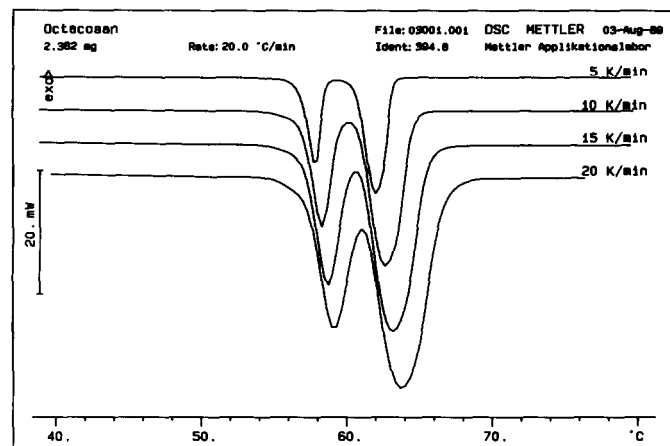


Fig. 4. DSC curve of octacosane, various heating rates.

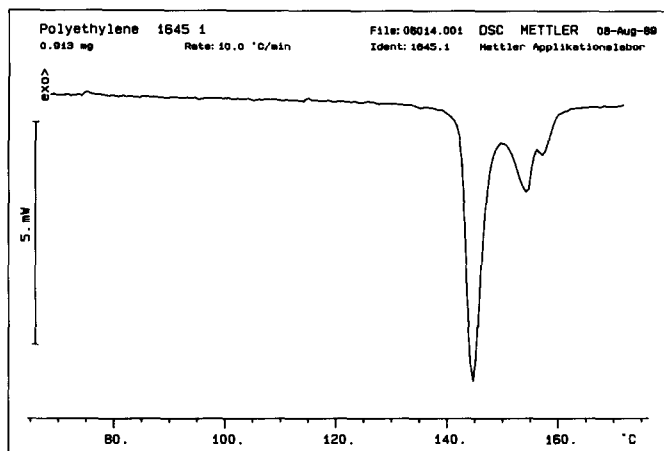


Fig. 5. DSC curve of PE fibre.

behaviour is very different when compared with randomly configured polyethylene. The melting peak not only shifted towards a higher temperature (in general  $> 145^{\circ}\text{C}$ ), but also more endotherms are usually present, caused by, e.g., internal stresses in the sample. These peaks in general are very close to each other. Figure 5 also illustrates that with a low sample weight, 0.913 mg., a good signal-to-noise ratio and peak resolution are obtained.

## CONCLUSIONS

The heat-flux DSC sensor described here combines a high sensitivity with a low signal time constant. By its high performance, the sensor is capable of all R & D and QC applications. Combined with the outstanding baseline quality inherent to the heat-flux principle, it is believed that this sensor provides the optimum solution in differential scanning calorimetry.

The new Mettler DSC 25 measuring cell will be provided with a sensor according to this technology as standard. At a later date replacement sensors for the Mettler DSC 20 and 30 cells will also become available.

## REFERENCES

- 1 G. van der Plaats, *Thermochim. Acta*, 72 (1984) 77.